

Synthesis and Antimycobacterial Evaluation of Novel Phthalazin-4-ylacetamides Against log- and Starved Phase Cultures

Dharmarajan Sriram*, Perumal Yogeeswari, Palaniappan Senthilkumar, Dewakar Sangaraju, Rohit Nelli, Debjani Banerjee, Pritesh Bhat and Thimmappa H. Manjashetty

Medicinal Chemistry & Antimycobacterial Research Laboratory, Pharmacy Group, Birla Institute of Technology & Science – Pilani, Hyderabad Campus, Jawahar Nagar, Hyderabad – 500 078, Andhra Pradesh, India

*Corresponding author: Dharmarajan Sriram, dsriram@bits-pilani.ac.in, drdsriram@yahoo.com

Twenty four novel 2-[3-(4-bromo-2-fluorobenzyl)-4-oxo-3,4-dihydro-1-phthalazinyl]acetic acid amides were synthesized from phthalic anhydride and were subjected to *in vitro* and *in vivo* evaluation against log- and starved phase of mycobacterial species and *Mycobacterium tuberculosis* isocitrate lyase enzyme inhibition studies. Among the compounds screened, 2-(2-(4-bromo-2-fluorobenzyl)-1,2-dihydro-1-oxophthalazin-4-yl)-N-(2,6-dimethylphenyl)acetamide (5j) inhibited all eight mycobacterial species with MIC's ranging from 0.08 to 5.05 μ M and was non-toxic to Vero cells till 126.43 μ M. Four compounds were tested against starved culture of *Mycobacterium tuberculosis* and they inhibited with MIC's ranging from 3.78 to 23.2 μ M. Some compounds showed 40–66% inhibition against *Mycobacterium tuberculosis* isocitrate lyase enzyme at 10 μ M. The docking studies also confirmed the binding potential of the compounds at the isocitrate lyase active site. In the *in vivo* animal model, 5j reduced the mycobacterial load in lung and spleen tissues with 1.38 and 2.9-log₁₀ protections, respectively, at 25 mg/kg body weight dose.

Key words: acetamides, antimycobacterial activity, antitubercular activity, dormant tuberculosis, isocitrate lyase enzyme, phthalazinyl derivatives, tuberculosis

Received 27 January 2009, revised 26 December 2009 and accepted for publication 31 December 2009

Mycobacterium tuberculosis (MTB) infects about 32% of the world's population. Every year, approximately 8 million of these infected people develop active tuberculosis (TB) and almost 2 million of these

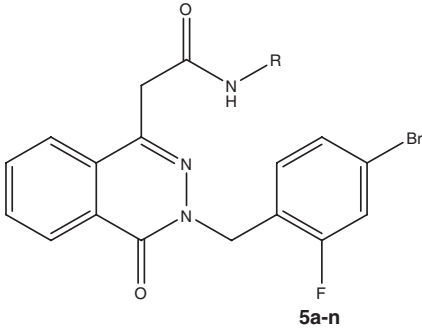
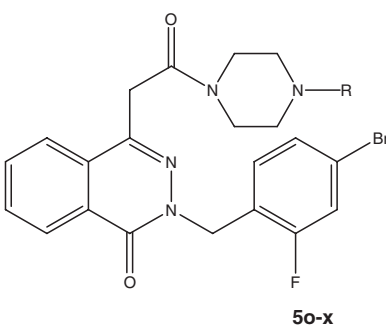
will die from the disease (1). Current chemotherapy for TB largely relies on drugs that inhibit bacterial metabolism with a heavy emphasis on inhibitors of the cell wall synthesis (2). According to their mode of action, first and second line TB drugs can be grouped as cell wall inhibitors [isonizide (INH), ethambutol, ethionamide, cycloserine], nucleic acid synthesis inhibitors [rifampicin (RIF), fluoroquinolones], protein synthesis inhibitors (streptomycin, kanamycin), and inhibitors of membrane energy metabolism [pyrazinamide (PAZ)]. Current TB drugs are mainly active against growing MTB, except for RIF and PAZ. RIF is active against both actively growing and slowly metabolizing non-growing MTB, whereas Pyrazinamide (PZA) is active against semi-dormant non-growing MTB in an acidic environment (3), such as in active inflammation sites in the lesions. These two agents are important sterilizing drugs that significantly reduce the number of MTB in infected tissues and shorten the therapy from 12 to 18 months to 6 months. Despite this, there are still persistent MTB populations that are not killed by any of these TB drugs. Therefore, drugs active against slowly growing or non-growing persistent bacilli are thought to be important to achieve a shortened therapy. A new TB treatment should offer at least one of three improvements over the existing regimens: (i) shorten the total duration of effective treatment and/or significantly reduce the total number of doses needed to be taken under Directly Observed Treatment, Short course (DOTS) supervision; (ii) improve the treatment of multi-drug resistant MTB (MDR-TB)/extensive drug resistant MTB (XDR-TB), which cannot be treated with INH and RIF and/or (iii) provide more effective treatment of latent TB infection, which is essential for eliminating TB. In the course of screening to discover new antimycobacterial compounds (4–13), we identified 2-[3-(4-bromo-2-fluorobenzyl)-4-oxo-3,4-dihydro-1-phthalazinyl]acetamides that inhibited *in vitro* *M. tuberculosis* H₃₇Rv (MTB) (log-phase and dormant phase), multi-drug resistant *M. tuberculosis* (MDR-TB), and various non-tuberculous mycobacteria (NTM). We present herein the results concerning the synthesis and the *in vitro* and *in vivo* antimycobacterial activities and MTB isocitrate lyase (ICL) enzyme inhibition studies of the representative compound of this phthalazine family. Docking studies also confirmed their binding potential at the ICL active site pocket in comparison with that reported for known inhibitor bromopyruvate.

Results and discussion

Synthesis

2-[3-(4-Bromo-2-fluorobenzyl)-4-oxo-3,4-dihydro-1-phthalazinyl]acetamides **5a–x** described in this study are shown in Table 1, and a reaction sequence for the preparation is outlined in Figure 1. The

Table 1: Antimycobacterial and cytotoxicities of phthalazin-4-ylacetamides

5a-n			5o-x							
										
			Minimum inhibitory concentration (μM)							
Compound no.	R	IC ₅₀ ^a (μM)	MTB ^b	MDR TB ^c	MS ^d	MM ^e	MV ^f	MP ^g	MF ^h	MK ⁱ
5a	Phenyl	NT ^j	6.71	NT	26.81	53.61	26.81	26.81	1.67	3.35
5b	4-Fluorophenyl	NT	6.46	NT	25.81	51.62	51.62	6.46	1.61	12.91
5c	4-Chlorophenyl	>124.81	3.12	3.12	12.48	49.93	24.96	1.56	12.48	3.12
5d	4-Bromophenyl	>114.64	2.86	1.43	1.43	45.85	1.43	11.46	1.43	5.74
5e	2-Trifluoromethylphenyl	116.98	2.92	2.92	93.58	23.39	11.69	2.92	11.69	5.86
5f	2-Chloro-5-trifluoromethylphenyl	NT	5.50	NT	5.50	43.96	10.99	1.37	2.74	5.50
5g	2-Methyl-3-chlorophenyl	>121.41	1.52	0.76	24.28	24.28	48.57	12.14	24.28	12.14
5h	4-Bromo-5-methylphenyl	NT	5.59	NT	89.41	44.70	22.35	11.18	22.35	11.18
5i	2,4-Dimethylphenyl	>126.43	0.79	0.38	3.16	50.57	12.64	6.33	3.16	6.33
5j	2,6-Dimethylphenyl	>126.43	0.18	0.08	1.58	1.58	50.57	1.58	3.16	1.58
5k	2-Pyridyl	NT	13.38	NT	106.9	53.50	6.69	13.38	26.75	53.50
5l	5-Methyl-2-pyridyl	<129.85	3.24	3.24	12.99	103.9	51.94	3.24	1.62	12.99
5m	6-Nitrobenzothiazol-2-yl	NT	5.51	NT	21.99	87.97	43.99	10.99	2.74	21.99
5n	5-Nitrothiazol-2-yl	NT	6.04	NT	24.12	96.47	24.12	3.01	3.01	24.12
5o	Methyl	NT	26.41	NT	105.6	52.82	105.6	6.61	6.61	26.41
5p	Phenyl	NT	11.67	NT	93.39	46.69	23.35	1.46	1.46	46.69
5q	4-Fluorophenyl	NT	5.66	NT	45.18	45.18	2.82	22.59	1.41	22.59
5r	4-Bromophenyl	NT	5.49	NT	43.87	43.87	43.87	2.74	1.37	43.87
5s	3-Trifluoromethylphenyl	NT	5.19	NT	5.19	41.43	20.72	5.19	2.59	10.36
5t	4-Methoxyphenyl	>110.54	2.76	1.38	11.05	44.21	44.21	2.76	5.54	22.11
5u	3-Methoxyphenyl	>110.54	2.76	2.76	11.05	44.21	44.21	2.76	1.38	44.21
5v	Benzyl	113.75	2.84	5.69	22.75	91.00	22.75	11.38	11.38	1.42
5w	2-Pyridyl	<116.52	1.45	1.45	11.65	46.61	46.61	5.84	11.65	1.45
5x	Piperonyl	102.89	2.57	2.57	20.58	82.31	41.16	5.15	5.15	10.29
Ciprofloxacin		>188.59	4.71	37.68	2.35	2.35	4.71	4.71	4.71	9.45
Rifampicin		>75.94	0.23	3.79	1.89	30.38	3.80	30.38	1.89	7.59
Isoniazid		>455.73	0.66	45.57	45.57	22.82	182.3	91.15	22.82	182.3

^aCytotoxicity in mammalian vero cell lines.^b*Mycobacterium tuberculosis*.^cMulti-drug resistant tuberculosis.^d*Mycobacterium smegmatis*.^e*Mycobacterium microti*.^f*Mycobacterium vaccae*.^g*Mycobacterium phlei*.^h*Mycobacterium fortuitum*.ⁱ*Mycobacterium kansasii*.^jNot tested.

first step, where phthalic anhydride (**1**) was reacted with ethyl 2-(1,1,1-triphenyl- λ^5 -phosphanylidene)acetate, to give ethyl 2-(3-oxo-1,3-dihydro-1-isobenzofuranylidene)acetate (**2**). The reaction proceeds via a diionic compound called a betaine, as an intermediate, which

forms oxaphosphetane that cleaves to form triphenylphosphine oxide and the corresponding olefin (14). Ethyl 2-(4-oxo-3,4-dihydro-1-phthalazinyl)acetate (**3**) was prepared by the condensation of 1 mole equivalent of **2** and 0.8 mole equivalent of hydrazine hydrate

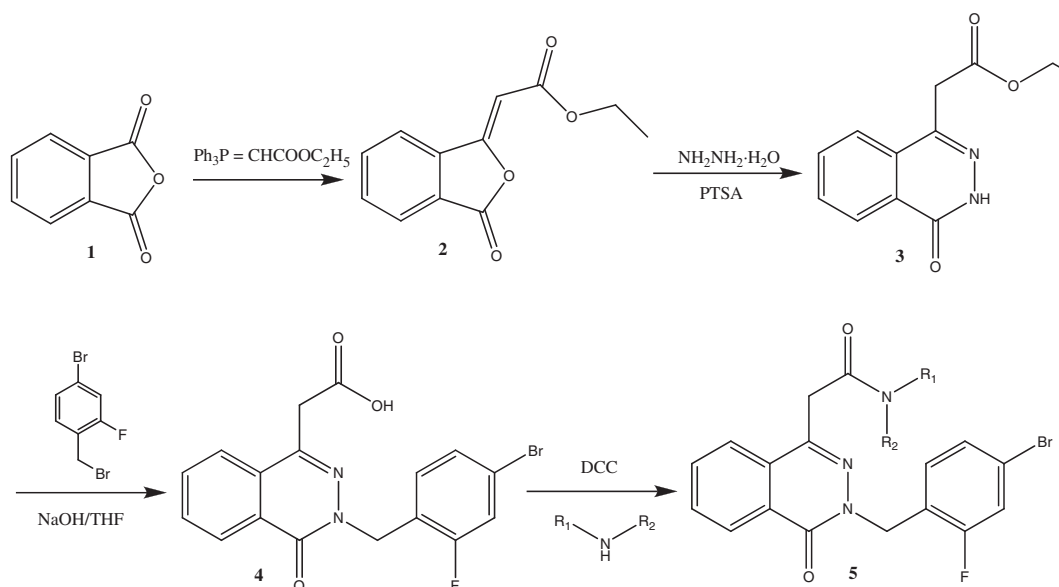


Figure 1: Synthetic protocol of the compounds.

using *p*-toluenesulphonic acid as a catalyst at room temperature for 8 min. There are a number of methods for synthesizing phthalazine nucleus (15) by refluxing phthalic anhydride and hydrazine hydrate, and these methods are not very satisfactory because of drawbacks such as high temperature, long reaction time (6 h), low yields (30–40%), effluent pollution and tedious workup procedure. In the present work using *p*-toluenesulphonic acid as a catalyst, the reaction proceeded efficiently at room temperature with excellent yield (86%) and in a state of high purity. Compound **3** on N-alkylation with 4-bromo-1-bromomethyl-2-fluoro benzene in the presence of sodium hydroxide yielded 2-[3-(4-bromo-2-fluorobenzyl)-4-oxo-3,4-dihydro-1-phthalazinyl]acetic acid (**4**). The base treatment also hydrolyzed the ethyl ester into free acid. Target compounds were prepared by condensing the acid **4** with corresponding amines in presence of dicyclohexyl carbodiimide (DCC). The purity of the synthesized compounds was monitored by thin layer chromatography (TLC) and elemental analyses, and the structures were identified by spectral data.

In vitro antimycobacterial activity

In the first phase, the compounds were screened for their *in vitro* antimycobacterial activity (16) against log-phase cultures of MTB, MDR-TB, and NTM like *Mycobacterium smegmatis* ATCC 14468, *Mycobacterium microti* MTCC 1727, *Mycobacterium vaccae* MTCC 997, *Mycobacterium phlei* MTCC 1724, *Mycobacterium fortuitum* MTCC 951, and *Mycobacterium kansasii* MTCC 3058 and MIC's of the synthesized compounds along with the standard drugs for comparison are reported (Table 1).

In the initial screening against MTB, the newer compounds showed good activity with MIC's ranging from 0.18 to 26.41 μM . Two compounds (**5i-j**) showed excellent activity with MIC of <1 μM . When compared to INH (MIC: 0.66 μM), one compounds (**5j**) was found to be more active with MIC of 0.18 μM . Compound **5j** was also found

to be more active than RIF (MIC: 0.23 μM). Twelve compounds were more potent than ciprofloxacin (MIC: 4.71 μM). Compound 2-(2-(4-bromo-2-fluorobenzyl)-1,2-dihydro-1-oxophthalazin-4-yl)-*N*-(2,6-dimethylphenyl)acetamide (**5j**) was found to be the most active compound *in vitro* with MIC's of 0.18 μM against MTB and was 3.6 and 1.2 times more potent than INH and RIF, respectively. With respect to structure-MTB activity, among the phthalazin-4-ylacetamides derived from phenyl derivatives (**5a-j**), any substituent in the phenyl ring enhances the activity (**5a** versus **5b-j**). Substituent with electron donating group like methyl enhanced the activity (**5i-j**). Amides derived from heterocyclic derivatives (**5k-n**) generally reduce the activity when compared to simple phenyl ring system. Most importantly against MDR-TB, when compared to INH (MIC 45.57 μM) and ciprofloxacin (MIC 37.68 μM), all the eleven compounds that screened were more active with MIC's in the range of 0.08–5.69 μM . Some compounds (**5d**, **5g**, **5i-j**, and **5t**) endowed greater activity toward the MDR-TB than MTB. Compound **5j** was found to be the most active compound and was 47, 471, and 569 times more potent than RIF, ciprofloxacin, and INH, respectively. All the compounds were also screened for atypical mycobacteria (AM), AM infection (17) an illness caused by a type of mycobacterium other than TB, which cause a wide variety of infections such as abscesses, septic arthritis, and osteomyelitis (bone infection). They can also infect the lungs, lymph nodes, gastrointestinal tract, skin, and soft tissues. The rate of AM infections is rare, but it is increasing as the AIDS population grows. Populations at risk include individuals who have lung disease and weakened immune systems. The synthesized compounds inhibited *M. smegmatis* (MS) with MIC's ranging from 1.58 to 106.9 μM , and eighteen compounds were more potent than INH (MIC: 45.57 μM); MS infects lungs (18). With regard to activity against *M. microti* (which causes sepsis tuberculosis acutissima in immuno-competent persons (19)), the compounds showed activity with MIC's ranging from 1.58 to 91.0 μM , and only one compound (**5j**) was more potent than INH (MIC: 22.82 μM). *M. vaccae*, which causes cutaneous and pulmonary

infections (20), was inhibited by the synthesized compounds with MIC's ranging from 1.43 to 51.62 μM , and all the compounds were more potent than INH (MIC: 182.3 μM). All the compounds also inhibited *M. phlei* (MP) that causes abscesses (21) with MIC's ranging from 1.37 to 26.81 μM and were more potent than INH (MIC: 91.15 μM). Against *M. fortuitum* (which causes infection in immuno-competent persons (22)), the compounds showed excellent activity with MIC's ranging from 1.37 to 26.75 μM , and twenty-three compounds were more potent than INH (MIC: 22.82 μM). The compounds were also screened against *M. kansasii* that causes central nervous system infection and cutaneous lymphadenitis (23), was inhibited with MIC's ranging from 1.42 to 53.50 μM , and all compounds were more potent than INH (MIC: 182.3 μM). Compound **5j** inhibited all the eight mycobacterium species with MIC ranging from 0.08 to 25.28 μM and was more potent than INH.

Starved MTB activity

The compounds that showed good activity against log-phase culture of MTB with MIC of less than 2 μM were further screened against 6-week-starved cells of MTB according to the literature procedure (24). Several *in vitro* model systems have been proposed to mimic the conditions found in the human chronic tuberculosis lesion (a granuloma), including oxygen starvation (25) nutrient deprivation (26), and rifampicin-induced persistence (27). Development of a screen under carbon-starvation conditions is feasible and less challenging than for oxygen deprivation. Prolonged deprivation of nutrients results in a marked slowing of bacterial growth and concomitant phenotypic antibiotic resistance (26). As bacteria can easily grow upon being returned to nutrient-rich media, this model allows easy quantification of antibiotic effectiveness. Against MTB, four compounds were tested, and they inhibited starved culture of MTB with MIC's ranging from 3.78 to 23.2 μM (Table 2). INH had poor activity against starved cells with MIC of 729.1 μM . As previously observed (24), RIF retained activity, although it is considerably less active against non-growing than against log-phase cells. All the four tested compounds were more potent than INH and two compounds (**5i-j**) were more potent than RIF (MIC: 15.2 μM). The presence of persistent and dormant MTB is thought to be the cause for the lengthy TB chemotherapy, because the current TB drugs are not effective in eliminating persistent or dormant bacilli. Therefore, these drugs active against slowly growing or non-growing persistent bacilli are thought to be important to achieve a shortened therapy.

Table 2: Inhibitory activities of selected compounds against log-phase and 6-week-starved *Mycobacterium tuberculosis* H37Rv

No	MIC in μM against MTB	
	Log-phase cells	6-Week-starved cells
5g	1.52	21.28
5i	0.79	15.01
5j	0.18	3.78
5w	1.45	23.2
Isoniazid	0.66	729.10
Rifampin	0.23	15.20

MTB, *Mycobacterium tuberculosis*.

ICL enzyme inhibition studies

Mycobacterial persistence refers to the ability of tubercle bacillus to survive in the face of chemotherapy and/or immunity (28). The nature of the persistent bacteria is unclear but might consist of stationary phase bacteria, postchemotherapy residual survivors and/or dormant bacteria that do not form colonies upon plating (29). The presence of such persistent bacteria is considered to be the major reason for lengthy therapy (30). A lot of research activity is currently aimed at understanding the biology of persistence of the tubercle bacillus and developing new drugs that target the persisters bacteria (31). Gene products involved in mycobacterial persistence, such as ICL (32), PcaA (methyl transferase involved in the modification of mycolic acid) (33), RelA (ppGpp synthase) (34), and DosR (controlling a 48-gene regulation involved in mycobacterial survival under hypoxic conditions) (35), have been identified and could be good targets for the development of drugs that target persistent bacilli. As these synthesized compounds showed activity against dormant mycobacterium, we decided to explore the possible mechanism by screening some compounds against ICL enzyme of MTB. ICL is an important enzyme in the glyoxylate cycle during carbohydrate starvation in MTB, and it catalyzes the cleavage of isocitrate to glyoxylate and succinate, allowing the organisms to survive on acetate or fatty acids (32). The glyoxylate cycle is not present in higher animals, and because of its necessity for survival for the persistent phase of the infection, ICL is considered an ideal drug target for persistent MTB. Several small-molecule inhibitors have been described (36) as MTB ICL inhibitors; however, none has been developed as a drug for MTB. The compounds were screened with a single concentration of 10 μM by standard protocol (37) and percentage inhibition of the screened compounds along with the standard MTB ICL inhibitor 3-nitropropionic acid (3-NP) (at 100 μM) for comparison are reported (Table 3). All the four compounds inhibited MTB ICL with percentage inhibition ranging from 40.62 to 66.70 at 10 μM . Two compounds (**5j** and **5w**) showed more than 50% inhibition, and all these compounds were found to be more potent than standard 3-NP at the dose level tested. Compound 2-(4-bromo-2-fluorobenzyl)-4-(2-oxo-2-(4-pyridin-2-yl)perazin-1-yl)ethylphthalazin-1(2H)-one (**5w**) was found to be the most active compound in the enzyme inhibition studies. This is the first report that screens newer synthetic compounds, which have an inhibition to MTB ICL. Further investigation could provide lead compounds for drug development against persistent TB.

Table 3: Inhibitory activities of selected compounds and 3-nitropropionic acid against MTB ICL

No	% Inhibition (μM)
5g	40.62 (10)
5i	48.34 (10)
5j	61.76 (10)
5w	66.70 (10)
3-NP	68.2 (100)
BP	52.1 (100)

ICL, isocitrate lyase; MTB, *Mycobacterium tuberculosis*; NP, nitropropionic acid.

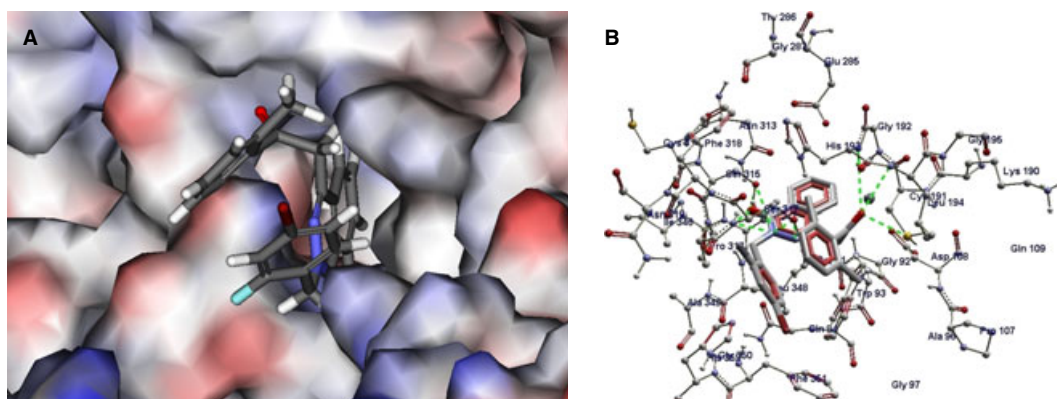


Figure 2: (A) Electrostatic surface map of MTB ICL with docked ligand inside the active site pocket of enzyme. (B) Binding mode of ligand with the MTB ICL. Only the residues in the active site were shown (residues within a distance of less than 10.0 Å are shown), hydrogen bonds are displayed by dotted green lines; Mg⁺⁺ is shown as black sphere.

Docking studies

The crystal structure of MTB ICL with bound inhibitor, bromopyruvate taken from the Protein Data Bank (PDB entry 1F8M) was used for docking the most active compound **5j**. MolDock showed good binding and interaction pattern for the ligand. There was a combined electrostatic and hydrophobic interaction pattern (Figure 2A) observed upon docking of the ligand with MTB ICL. The ligand manifested multicenter H-bond (Figure 2B) between the C=O of dimethylbenzyl group and SH of Cys 191 (SH...C=O, 3.31 Å), Leu 194 (NH...C=O, 3.35 Å), His 193 (NH...C=O, 3.2 Å). Trifurcated hydrogen bonding was observed between C=O group phthalazine-1-one and Ser 315 (OH...C=O, 2.41 Å), Ser 317 (NH...C=O, 3.42 Å) and Thr 347 (OH...C=O, 2.56 Å). Another multicentric trifurcated hydrogen bonding was seen at N1 of phthalazine-1-one with Ser 315 (OH...N1, 3.01 Å), Ser 317 (OH...N1, 2.71 Å; NH...N1 2.98 Å). Hydrogen bonding was also seen between Ser 317 and N2 of phthalazine-1-one (OH...N2, 2.89 Å). Even though internal stabilization by *pi-pi* staking was seen between dimethylbenzyl group and 4-bromo-2-fluorobenzyl groups, external stabilization by hydrophobic interactions also has been observed. Van der Waals interactions were seen between the 4-bromo-2-fluorobenzyl moiety and His 352 (3.43 Å), and a hydrophobic interaction with Pro 316 (3.02 Å). The hydrophobic pocket formed by Trp 93 and Leu 194 was found to stabilize the dimethylbenzyl moiety. The hydrophobic pocket formed by side chains of amino acid residues Trp 93, Cys 191, Thr 347, and Leu 348 were found to stabilize the phthalazine moiety. There were many common interaction residues observed for the ligand on docking in comparison with the interaction pattern observed for bromopyruvate and nitropropionate crystallized with MTB ICL (38). The most important amino acid residue involved in the case of bromopyruvate is Cys 191, with which it forms an irreversible covalent adduct and thus inactivates the enzyme. Other than this, bromopyruvate forms hydrogen bond with side chain of amino acid residues His 193, Ser 315, Ser 317, and Thr 347. The same amino acid residues have been observed to form hydrogen bonding with nitropropionate also. There were common amino acid residues showing the hydrophobic stabilization for our ligand (**5j**) and nitropropionate. They

Table 4: *In vivo* activity data of **5j** and INH against *Mycobacterium tuberculosis* ATCC 35801 in mice at 25 mg/kg

Compound	Lungs (log CFU \pm SEM)	Spleen (log CFU \pm SEM)
Control	7.99 \pm 0.16	9.02 \pm 0.21
Isoniazid	5.86 \pm 0.23	4.71 \pm 0.10
5j	6.61 \pm 0.18	6.12 \pm 0.21

INH, isonizide.

were Trp 93, Thr 347, and Leu 348. This suggests that the compound **5j** has good affinity for the enzyme.

Cytotoxicity

Some compounds were further examined for toxicity (IC₅₀) in a mammalian Vero cell line at concentrations of 62.5 μ g/mL (Table 1) (39). The compounds with pyridyl derivatives were found to be toxic, which is followed by aryl piperazinyl substituted derivatives and phenyl substituted derivatives show no or less toxicity. These results are important as these compounds with their decreased cytotoxicity are much better attractive in the development of compounds for the treatment of TB. This is primarily because of the fact that the eradication of TB requires a lengthy course of treatment, and the need for an agent with a high margin of safety becomes a primary concern. Compound **5j** showed selectivity index (IC₅₀/MIC) of more than 702 and 1580 against log-phase MTB and MDR-TB infections. For the persistent culture of MTB, the selectivity index of compound **5j** is 33.

In vivo antimycobacterial activity

Subsequently, compound **5j** was tested for efficacy against MTB at a dose of 25 mg/Kg (Table 4) in six-week-old female CD-1 mice (11,40). In this model, the mice were infected with *M. tuberculosis* ATCC 35801 and drug treatment began after inoculation of the animal with microorganism for 10 days. After 35 days post infection, the spleens and right lungs were aseptically removed and bacterial counts were measured, and compared with the

counts from negative (untreated) controls (mean culture forming units (CFU) in lung: 7.99 ± 0.16 and in spleen: 9.02 ± 0.21). Compound **5j** decreased the bacterial load in lung and spleen tissues with 1.38 and 2.9-log₁₀ protections, respectively, and was considered to be promising in reducing bacterial count in lung and spleen tissues. When compared to INH at the same dose level, **5j** was found to be less active in the *in vivo* study. The reason for this less *in vivo* activity might be because of the instability of the compounds, as it gets hydrolyzed in to the less active acetic acid intermediate 2-[3-(4-bromo-2-fluorobenzyl)-4-oxo-3,4-dihydro-1-phthalazinyl]acetic acid (**4**) that showed *in vitro* MIC of 25.0 µg/mL against MTB.

Conclusion

Screening of the antimycobacterial activity of these novel series identified 2-[3-(4-bromo-2-fluorobenzyl)-4-oxo-3,4-dihydro-1-phthalazinyl]acetamides as a new lead endowed with high activity toward MTB, MDR-TB, NTM, dormant MTB, and ICL of MTB. The present study reveals the importance of these compounds effective for the treatment of TB, MDR-TB, persistent TB, and NTM infections. Overall activity profile of **5j** is more pronounced in the paper because of the high activity profile with respect to MIC and enzyme activity. 5w activity profile indicates comparable enzyme inhibition compared to MIC. The possible reason could be because of lack of membrane penetration of 5w when compared to **5j**, which needs further studies to assess these concepts. The most active compound showed binding affinity comparable with that of known inhibitors as seen with the docked residues. In conclusion, it has been shown that the potency, selectivity, and low cytotoxicity of these compounds make them valid leads for synthesizing new compounds that possess better activity. Further structure-activity and mechanistic studies should prove fruitful.

Experimental section

Melting points were taken on an electrothermal melting point apparatus (Buchi BM530) in open capillary tubes and are uncorrected ¹H-NMR spectra were scanned on a JEOL Fx 400MHz NMR spectrometer using CDCl₃, DMSO-d₆ as solvent. Chemical shifts are expressed in δ (ppm) relative to tertamethylsilane. Elemental analyses (C, H, and N) were performed on Perkin Elmer model 240C analyzer and the data were within ±0.4% of the theoretical values. The use of animals for the experimental purpose has been approved by Institutional Animal Ethics Committee (IAEC) (Protocol no. IAEC/RES/11 on 21/04/2003 and extended till 20/04/2009).

Synthesis of ethyl 2-(3-oxo-1,3-dihydro-1-isoben-7zofuranylidene)acetate (**2**)

A solution of phthalic anhydride (1.0 equiv.) and ethyl 2-(1,1,1-triphenyl-λ⁵-phosphanylidene)acetate (1.1 equiv.) in 300 mL of dichloromethane (DCM) was refluxed for 3 h. DCM was removed by vacuum at 40–50 °C. To the resulting sticky solid, 2 × 150 mL of hexane was added, stirred for 10 min, and the unreacted 2-(1,1,1-triphenyl-λ⁵-phosphanylidene)acetate was removed by

filtration. The organic solvent was removed under vacuum and the resulting crude semisolid was taken to next step without further purification. Yield: 84%. ¹H-NMR CDCl₃; δ (ppm): 1.1 (t, 3H), 4.2 (q, 2H), 6.0 (s, 1H), 7.6 (t, 1H), 7.7 (t, 1H), 7.8 (d, 1H), 8.9 (d, 1H).

Synthesis of ethyl 2-(4-oxo-3,4-dihydro-1-phthalazinyl)acetate (**3**)

A mixture of **2** (1.0 equiv.), hydrazine hydrate (0.8 equiv) and para toluene sulphonic acid (PTSA) (1.0 equiv.) was ground by pestle and mortar at room temperature for 8 min. On completion, as indicated by TLC, the reaction mixture was treated with water. The resultant product was filtered, washed with water and recrystallized from DMF to give **3** in high yields (86%). ¹H-NMR CDCl₃; δ (ppm): 1.1 (t, 3H), 3.9 (s, 2H), 4.1 (q, 2H), 7.6 (t, 1H), 7.7 (t, 1H), 7.8 (t, 1H), 8.3–8.4 (d, 1H), 10.0 (s, 1H).

Synthesis of 2-[3-(4-bromo-2-fluorobenzyl)-4-oxo-3,4-dihydro-1-phthalazinyl]acetic acid (**4**)

A mixture of **3** (1.0 equiv.), NaOH (5.0 equiv.), and tetrahydrofuran (THF) was stirred for 30 min at 40–50 °C. 4-bromo-1-bromomethyl-2-fluoro benzene (1.1 equiv.) was added to the reaction mixture and stirred for 2 h at 50–60 °C. Water was added to the reaction mixture and stirred at room temperature for 1 h. pH was adjusted to 2–3 using cold acetic acid. THF was removed and the aqueous phase was extracted with ethyl acetate (2 × 50 mL), washed with brine, dried over sodium sulfate, and evaporated. The solid was crystallized with methanol to give **4** with 54% yield. ¹H-NMR (DMSO-d₆); δ (ppm): 3.98 (s, 2H), 5.3 (s, 2H), 7.17 (t, 1H), 7.35 (dd, 1H, J₁ = 8.0, J₂ = 1.6), 7.55 (dd, 1H, J₁ = 8.0, J₂ = 1.6), 7.87 (t, 1H), 7.9 (t, 1H), 7.95 (t, 1H), 8.29 (d, 1H).

General procedure for the synthesis of 2-[2-(4-bromo-2-fluorobenzyl)-1,2-dihydro-1-oxophthalazin-4-yl]-N-(substituted) amides (**5a–x**)

Compound **4** (1 equiv.) and DCC (1.1 equiv.) were taken in a round-bottom flask with dichloromethane as solvent and stirred at a temperature of 0–4 °C for 30 min. Then added equimolar amount of appropriate primary or secondary amine and stirred for 8–10 h. The reaction progress was monitored by TLC using a mixture of ethyl acetate: hexane (1:1) as the mobile phase. After the reaction, the precipitate of urea obtained was filtered off, and the DCM layer was washed with water. Then the DCM layer was collected; and to this, sodium sulphate was added to remove traces of water. Then, the DCM was distilled off to get the residue of **5** with 44–90% yield.

2-(2-(4-Bromo-2-fluorobenzyl)-1,2-dihydro-1-oxophthalazin-4-yl)-N-phenylacetamide (**5a**)

Yield: 86%; m.p.: 197 °C; ¹H-NMR (DMSO-d₆) δ (ppm): 4.01 (s, 2H), 5.32 (s, 2H), 7.2–8.2 (m, 12H), 12.01 (s, 1H); ¹³C NMR (DMSO-d₆) δ (ppm): 186.8, 161.7, 158.7, 141.3, 139.2, 132.3, 131.2, 130.7, 129.8, 129.2, 127.6, 127.1, 124.5, 122.7, 121.8, 120.5, 38.9; Anal: C₂₃H₁₇BrFN₃O₂, C, H, N.

2-(2-(4-Bromo-2-fluorobenzyl)-1,2-dihydro-1-oxo phthalazin-4-yl)-N-(4-fluorophenyl)acetamide (5b)

Yield: 82%; m.p.: 209 °C; ¹H-NMR (DMSO-d₆) δ (ppm): 3.98 (s, 2H), 5.33 (s, 2H), 7.4–8.19 (m, 11H), 12.0 (s, 1H); ¹³C NMR (DMSO-d₆) δ (ppm): 186.8, 161.7, 158.7, 141.3, 134.2, 132.3, 131.2, 130.7, 129.8, 129.2, 127.6, 127.1, 123.6, 122.7, 120.5, 115.9, 38.9; Anal: C₂₃H₁₆BrF₂N₃O₂, C, H, N.

2-(2-(4-Bromo-2-fluorobenzyl)-1,2-dihydro-1-oxo phthalazin-4-yl)-N-(4-chlorophenyl)acetamide (5c)

Yield: 90%; m.p.: 192 °C; ¹H-NMR (DMSO-d₆) δ (ppm): 3.99 (s, 2H), 5.33 (s, 2H), 7.4–8.18 (m, 11H), 12.0 (s, 1H); ¹³C NMR (DMSO-d₆) δ (ppm): 186.8, 161.7, 158.7, 141.3, 138.5, 132.3, 131.2, 130.7, 129.8, 129.2, 127.6, 127.1, 123.0, 122.7, 120.5, 38.9; Anal: C₂₃H₁₆BrClFN₃O₂, C, H, N.

2-(2-(4-Bromo-2-fluorobenzyl)-1,2-dihydro-1-oxo phthalazin-4-yl)-N-(4-bromophenyl)acetamide (5d)

Yield: 88%; m.p.: 208 °C; ¹H-NMR (DMSO-d₆) δ (ppm): 4.01 (s, 2H), 5.28 (s, 2H), 7.27–8.19 (m, 11H), 12.0 (s, 1H); ¹³C NMR (DMSO-d₆) δ (ppm): 186.8, 161.7, 158.7, 141.3, 138.2, 132.3, 131.9, 131.2, 130.7, 129.8, 129.2, 127.6, 127.1, 124.5, 122.7, 120.5, 119.5, 38.9; Anal: C₂₃H₁₆Br₂FN₃O₂, C, H, N.

2-(2-(4-Bromo-2-fluorobenzyl)-1,2-dihydro-1-oxo phthalazin-4-yl)-N-(2-trifluoromethylphenyl)acetamide (5e)

Yield: 81%; m.p.: 170 °C; ¹H-NMR (DMSO-d₆) δ (ppm): 4.01 (s, 2H), 5.33 (s, 2H), 7.15–8.67 (m, 11H), 12.0 (s, 1H); ¹³C NMR (DMSO-d₆) δ (ppm): 186.8, 161.7, 158.7, 141.3, 134.5, 132.3, 131.2, 130.7, 129.8, 129.2, 127.6, 127.1, 126.3, 125.6, 122.7, 120.5, 116.3, 38.9; Anal: C₂₄H₁₆BrF₄N₃O₂, C, H, N.

2-(2-(4-Bromo-2-fluorobenzyl)-1,2-dihydro-1-oxo phthalazin-4-yl)-N-(2-chloro-5-(trifluoromethyl)phenyl)acetamide (5f)

Yield: 85%; m.p.: 237 °C; ¹H-NMR (DMSO-d₆) δ (ppm): 3.98 (s, 2H), 5.30 (s, 2H), 7.13–8.18 (m, 10H), 12.0 (s, 1H); ¹³C NMR (DMSO-d₆) δ (ppm): 186.8, 161.7, 158.7, 141.3, 139.5, 134.5, 132.3, 131.2, 130.7, 129.8, 129.2, 127.6, 127.1, 124.5, 123.4, 122.7, 120.5, 38.9; Anal: C₂₄H₁₅BrClF₄N₃O₂, C, H, N.

2-(2-(4-Bromo-2-fluorobenzyl)-1,2-dihydro-1-oxo phthalazin-4-yl)-N-(2-methyl-3-chlorophenyl)acetamide (5g)

Yield: 80%; m.p.: 210 °C; ¹H-NMR (DMSO-d₆) δ (ppm): 3.98 (s, 2H), 5.32 (s, 2H), 7.34–8.18 (m, 10H), 12.0 (s, 1H); ¹³C NMR (DMSO-d₆) δ (ppm): 186.8, 161.7, 158.7, 141.3, 139.5, 136.6, 135.2, 132.3, 131.2, 130.7, 129.8, 129.2, 127.6, 127.1, 124.6, 122.7, 120.5, 38.9, 6.5; Anal: C₂₄H₁₆BrClFN₃O₂, C, H, N.

2-(2-(4-Bromo-2-fluorobenzyl)-1,2-dihydro-1-oxo phthalazin-4-yl)-N-(4-bromo-5-methylphenyl)acetamide (5h)

Yield: 82%; m.p.: 180 °C; ¹H-NMR (DMSO-d₆) δ (ppm): 3.98 (s, 2H), 5.33 (s, 2H), 7.27–8.38 (m, 10H), 12.0 (s, 1H); ¹³C NMR (DMSO-d₆) δ (ppm): 186.8, 161.7, 158.7, 141.3, 139.6, 138.2, 132.3, 131.9, 131.2, 130.7, 129.8, 129.2, 127.6, 127.1, 122.7, 121.3, 120.5, 119.9, 38.9, 16.3; Anal: C₂₄H₁₈Br₂FN₃O₂, C, H, N.

2-(2-(4-Bromo-2-fluorobenzyl)-1,2-dihydro-1-oxo phthalazin-4-yl)-N-(2,4-dimethylphenyl)acetamide (5i)

Yield: 80%; m.p.: 173 °C; ¹H-NMR (DMSO-d₆) δ (ppm): 4.01 (s, 2H), 5.31 (s, 2H), 7.28–8.39 (m, 10H), 12.0 (s, 1H); ¹³C NMR (DMSO-d₆) δ (ppm): 186.8, 161.7, 158.7, 141.3, 134.9, 134.6, 133.9, 132.3, 131.2, 130.7, 129.8, 129.2, 127.6, 127.1, 126.5, 122.7, 120.5, 38.9, 25.6, 16.5; Anal: C₂₅H₂₁BrFN₃O₂, C, H, N.

2-(2-(4-Bromo-2-fluorobenzyl)-1,2-dihydro-1-oxo phthalazin-4-yl)-N-(2,6-dimethylphenyl)acetamide (5j)

Yield: 83%; m.p.: 148 °C; ¹H-NMR (DMSO-d₆) δ (ppm): 3.99 (s, 2H), 5.33 (s, 2H), 7.27–8.38 (m, 10H), 12.0 (s, 1H); ¹³C NMR (DMSO-d₆) δ (ppm): 186.8, 161.7, 158.7, 141.3, 138.2, 135.2, 132.3, 131.2, 130.7, 129.8, 129.2, 127.6, 127.1, 126.6, 124.5, 122.7, 120.5, 38.9, 16.5; Anal: C₂₅H₂₁BrFN₃O₂, C, H, N.

2-(2-(4-Bromo-2-fluorobenzyl)-1,2-dihydro-1-oxophthalazin-4-yl)-N-(pyridin-2-yl)acetamide (5k)

Yield: 80%; m.p.: 172 °C; ¹H-NMR (DMSO-d₆) δ (ppm): 3.98 (s, 2H), 5.33 (s, 2H), 6.88–8.79 (m, 11H), 12.0 (s, 1H); ¹³C NMR (DMSO-d₆) δ (ppm): 186.8, 161.7, 158.7, 152.3, 147.4, 141.3, 138.9, 132.3, 131.2, 130.7, 129.8, 129.2, 127.6, 127.1, 122.7, 120.5, 119.6, 117.9, 38.9; Anal: C₂₂H₁₆BrFN₄O₂, C, H, N.

2-(2-(4-Bromo-2-fluorobenzyl)-1,2-dihydro-1-oxophthalazin-4-yl)-N-(4-methylpyridin-2-yl)acetamide (5l)

Yield: 65%; m.p.: 185 °C; ¹H-NMR (DMSO-d₆) δ (ppm): 3.98 (s, 2H), 5.33 (s, 2H), 7.15–8.69 (m, 10H), 12.0 (s, 1H); ¹³C NMR (DMSO-d₆) δ (ppm): 186.8, 161.7, 158.7, 150.9, 150.2, 147.5, 141.3, 132.3, 131.2, 130.7, 129.8, 129.2, 127.6, 127.1, 124.6, 122.7, 120.5, 38.9, 25.6; Anal: C₂₃H₁₈BrFN₄O₂, C, H, N.

2-(2-(4-Bromo-2-fluorobenzyl)-1,2-dihydro-1-oxophthalazin-4-yl)-N-(6-nitrobenzo[d]thiazol-2-yl)acetamide (5m)

Yield: 69%; m.p.: 152 °C; ¹H-NMR (DMSO-d₆) δ (ppm): 3.98 (s, 2H), 5.33 (s, 2H), 6.7–9.15 (m, 10H), 12.0 (s, 1H); ¹³C NMR (DMSO-d₆) δ (ppm): 190.2, 186.8, 161.7, 158.7, 156.2, 145.6, 141.3, 132.3, 131.2, 130.7, 129.8, 129.2, 127.6, 127.1, 125.6, 122.7, 120.5, 118.3, 38.9; Anal: C₂₄H₁₅BrFN₅O₄S, C, H, N.

2-(2-(4-Bromo-2-fluorobenzyl)-1,2-dihydro-1-oxo phthalazin-4-yl)-N-(5-nitrothiazol-2-yl)acetamide (5n)

Yield: 44%; m.p.: 171 °C; $^1\text{H-NMR}$ (DMSO- d_6) δ (ppm): 3.98 (s, 2H), 5.33 (s, 2H), 6.8–8.19 (m, 7H), 8.6 (s, 1H); 12.0 (s, 1H); ^{13}C NMR (DMSO- d_6) δ (ppm): 186.8, 165.9, 161.7, 158.7, 145.3, 141.3, 135.6, 132.3, 131.2, 130.7, 129.8, 129.2, 127.6, 127.1, 122.7, 120.5, 38.9; Anal: $\text{C}_{20}\text{H}_{13}\text{BrFN}_5\text{O}_4\text{S}$, C, H, N.

2-(2-(4-Bromo-2-fluorobenzyl)-4-(2-(4-methylpiperazin-1-yl)-2-oxoethyl)phthalazin-1(2H)-one (5o)

Yield: 55%; m.p.: 133 °C; $^1\text{H-NMR}$ (DMSO- d_6) δ (ppm): 2.59 (t, 4H), 2.78 (s, 1H), 3.12 (t, 4H), 3.98 (s, 2H), 5.33 (s, 2H), 6.90–8.08 (m, 7H); ^{13}C NMR (DMSO- d_6) δ (ppm): 186.8, 161.7, 158.7, 141.3, 132.3, 131.2, 130.7, 129.8, 129.2, 127.6, 127.1, 122.7, 120.5, 55.6, 47.6, 43.5, 38.9; Anal: $\text{C}_{22}\text{H}_{22}\text{BrFN}_4\text{O}_2$, C, H, N.

2-(2-(4-Bromo-2-fluorobenzyl)-4-(2-oxo-2-(4-phenylpiperazin-1-yl)phthalazin-1(2H)-one (5p)

Yield: 80%; m.p.: 198 °C; $^1\text{H-NMR}$ (DMSO- d_6) δ (ppm): 2.55 (s, 4H), 3.12 (t, 4H), 4.01 (s, 2H), 5.32 (s, 2H), 6.94–8.18 (m, 12H); ^{13}C NMR (DMSO- d_6) δ (ppm): 186.8, 161.7, 158.7, 149.5, 141.3, 132.3, 131.2, 130.7, 129.8, 129.2, 127.6, 127.1, 122.7, 120.5, 118.6, 114.8, 50.6, 47.5, 38.9; Anal: $\text{C}_{27}\text{H}_{24}\text{BrFN}_4\text{O}_2$, C, H, N.

2-(2-(4-Bromo-2-fluorobenzyl)-4-(2-(4-(4-fluorophenyl)piperazin-1-yl)-2-oxoethyl)phthalazin-1(2H)-one (5q)

Yield: 88%; m.p.: 191 °C; $^1\text{H-NMR}$ (DMSO- d_6) δ (ppm): 2.55 (s, 4H), 3.12 (t, 4H), 4.01 (s, 2H), 5.32 (s, 2H), 6.94–8.18 (m, 11H); ^{13}C NMR (DMSO- d_6) δ (ppm): 186.8, 161.7, 158.7, 152.2, 145.3, 141.3, 132.3, 131.2, 130.7, 129.8, 129.2, 127.6, 127.1, 122.7, 120.5, 116.5, 115.2, 50.6, 47.5, 38.9; Anal: $\text{C}_{27}\text{H}_{23}\text{BrF}_2\text{N}_4\text{O}_2$, C, H, N.

2-(2-(4-Bromo-2-fluorobenzyl)-4-(2-(4-(4-bromophenyl)piperazin-1-yl)-2-oxoethyl)phthalazin-1(2H)-one (5r)

Yield: 82%; m.p.: 174 °C; $^1\text{H-NMR}$ (DMSO- d_6) δ (ppm): 2.54 (s, 4H), 3.13 (t, 4H), 4.05 (s, 2H), 5.31 (s, 2H), 6.93–8.15 (m, 11H); ^{13}C NMR (DMSO- d_6) δ (ppm): 186.8, 161.7, 158.7, 149.3, 141.3, 132.8, 132.3, 131.2, 130.7, 129.8, 129.2, 127.6, 127.1, 122.7, 120.5, 116.8, 112.5, 50.6, 47.5, 38.9; Anal: $\text{C}_{27}\text{H}_{23}\text{Br}_2\text{FN}_4\text{O}_2$, C, H, N.

2-(2-(4-Bromo-2-fluorobenzyl)-4-(2-(4-(3-(trifluoromethyl)phenyl)piperazin-1-yl)-2-oxoethyl)phthalazin-1(2H)-one (5s)

Yield: 88%; m.p.: 208 °C; $^1\text{H-NMR}$ (DMSO- d_6) δ (ppm): 2.54 (s, 4H), 3.13 (t, 4H), 4.05 (s, 2H), 5.31 (s, 2H), 6.93–8.16 (m, 11H); ^{13}C NMR (DMSO- d_6) δ (ppm): 186.8, 161.7, 158.7, 150.5, 141.3, 132.3, 131.9, 131.2, 130.7, 129.8, 129.2, 127.6, 127.1, 124.2, 122.7, 120.5, 115.2, 110.4, 50.6, 47.5, 38.9; Anal: $\text{C}_{28}\text{H}_{23}\text{BrF}_4\text{N}_4\text{O}_2$, C, H, N.

2-(2-(4-Bromo-2-fluorobenzyl)-4-(2-(4-(4-methoxyphenyl)piperazin-1-yl)-2-oxoethyl)phthalazin-1(2H)-one (5t)

Yield: 89%; m.p.: 182 °C; $^1\text{H-NMR}$ (DMSO- d_6) δ (ppm): 2.54 (s, 4H), 3.13 (t, 4H), 3.75 (s, 3H), 4.05 (s, 2H), 5.31 (s, 2H), 6.93–8.15 (m, 11H); ^{13}C NMR (DMSO- d_6) δ (ppm): 186.8, 161.7, 158.7, 151.2, 142.5, 141.3, 132.3, 131.2, 130.7, 129.8, 129.2, 127.6, 127.1, 122.7, 120.5, 115.9, 115.2, 56.8, 50.6, 47.5, 38.9; Anal: $\text{C}_{28}\text{H}_{26}\text{BrFN}_4\text{O}_3$, C, H, N.

2-(2-(4-Bromo-2-fluorobenzyl)-4-(2-(4-(3-methoxyphenyl)piperazin-1-yl)-2-oxoethyl)phthalazin-1(2H)-one (5u)

Yield: 61%; m.p.: 153 °C; $^1\text{H-NMR}$ (DMSO- d_6) δ (ppm): 2.54 (s, 4H), 3.13 (t, 4H), 3.75 (s, 3H), 4.05 (s, 2H), 5.31 (s, 2H), 6.93–8.15 (m, 11H); ^{13}C NMR (DMSO- d_6) δ (ppm): 186.8, 162.5, 161.7, 158.7, 150.9, 141.3, 132.3, 131.2, 130.7, 129.8, 129.2, 127.6, 127.1, 122.7, 120.5, 103.2, 98.1, 50.6, 47.5, 38.9; Anal: $\text{C}_{28}\text{H}_{26}\text{BrFN}_4\text{O}_3$, C, H, N.

2-(2-(4-Bromo-2-fluorobenzyl)-4-(2-(4-benzylpiperazin-1-yl)-2-oxoethyl)phthalazin-1(2H)-one (5v)

Yield: 52%; m.p.: 119 °C; $^1\text{H-NMR}$ (DMSO- d_6) δ (ppm): 3.96 (s, 2H), 4.14 (s, 2H), 5.33 (s, 2H), 7.17–8.19 (m, 12H); ^{13}C NMR (DMSO- d_6) δ (ppm): 186.8, 161.7, 158.7, 141.3, 135.4, 132.3, 131.2, 130.7, 129.8, 129.2, 128.9, 128.1, 127.6, 127.8, 127.1, 122.7, 120.5, 61.2, 50.6, 47.5, 38.9; Anal: $\text{C}_{28}\text{H}_{26}\text{BrFN}_4\text{O}_2$, C, H, N.

2-(4-Bromo-2-fluorobenzyl)-4-(2-oxo-2-(4-pyridin-2-yl)piperazin-1-yl)ethyl)phthalazin-1(2H)-one (5w)

Yield: 60%; m.p.: 131 °C; $^1\text{H-NMR}$ (DMSO- d_6) δ (ppm): 2.55 (s, 4H), 3.12 (t, 4H), 4.01 (s, 2H), 5.32 (s, 2H), 6.94–8.18 (m, 11H); ^{13}C NMR (DMSO- d_6) δ (ppm): 186.8, 161.7, 158.7, 154.3, 148.7, 141.3, 138.9, 132.3, 131.2, 130.7, 129.8, 129.2, 127.6, 127.1, 122.7, 120.5, 114.2, 50.6, 47.5, 38.9; Anal: $\text{C}_{26}\text{H}_{23}\text{BrFN}_5\text{O}_2$, C, H, N.

2-(4-Bromo-2-fluorobenzyl)-4-(2-oxo-2-(4-piperonoyl)piperazin-1-yl)ethyl)phthalazin-1(2H)-one (5x)

Yield: 88%; m.p.: 141 °C; $^1\text{H-NMR}$ (DMSO- d_6) δ (ppm): 2.55 (s, 4H), 3.12 (t, 4H), 4.01 (s, 2H), 5.32 (s, 2H), 6.12 (s, 2H), 7.12–8.18 (m, 10H); ^{13}C NMR (DMSO- d_6) δ (ppm): 190.5, 186.8, 161.7, 158.7, 150.1, 148.4, 141.3, 132.3, 131.2, 130.7, 129.8, 129.2, 128.3, 127.6, 127.1, 122.7, 120.5, 115.3, 112.6, 101.3, 50.6, 47.5, 38.9; Anal: $\text{C}_{29}\text{H}_{24}\text{BrFN}_4\text{O}_5$, C, H, N.

Antimycobacterial activity in log-phase cultures

All compounds were screened for their *in vitro* antimycobacterial activity against log-phase cultures of MTB, MDR-TB, and NTM species like *M. smegmatis* ATCC 14468, *M. microti* MTCC 1727,

M. vaccae MTCC 997, *M. phlei* MTCC 1724, *M. fortuitum* MTCC 951, and *M. kansasii* MTCC 3058 in Middlebrook 7H11 agar medium supplemented with Oleic acid, Dextrose, Catalase (OADC) by agar dilution method similar to that recommended by the National Committee for Clinical Laboratory Standards for the determination of MIC in triplicates. The MDR-TB clinical isolate was obtained from Tuberculosis Research Center, Chennai, India, and was resistant to isoniazid, rifampicin, and ciprofloxacin. The minimum inhibitory concentration (MIC) is defined as the minimum concentration of compound required to give complete inhibition of bacterial growth.

Antimycobacterial activity in 6-week-starved cultures

For starvation experiments, MTB cells were grown in Middlebrook 7H9 medium supplemented with 0.2% (vol/vol) glycerol, 10% (vol/vol) Middlebrook oleic acid-albumin-dextrose-catalase (OADC) enrichment, and 0.025% (vol/vol) Tween 80 at 37 °C with constant rolling at 2 rpm until they reached an optical density at 600 nm of ~0.6. The cells were then washed twice and re-suspended in phosphate-buffered saline (PBS) at the same cell density. Cells (50 mL of culture) were incubated at 37 °C for an additional 6 weeks in 1-liter roller bottles. Compounds, dissolved in DMSO, were added to either 1 mL PBS containing $\sim 1 \times 10^7$ starved MTB cells at various concentrations. Cultures were incubated in 15-mL conical tubes at 37 °C with constant shaking for 7 days and then washed twice in PBS before dilutions were plated on Middlebrook 7H11 plates supplemented with 0.2% (vol/vol) glycerol, 10% (vol/vol) Middlebrook OADC enrichment, and 0.025% (vol/vol) Tween 80, containing no antibiotics. Bacterial growth was determined after incubation for 4 weeks at 37 °C. The minimum inhibitory concentration (MIC) is defined as the minimum concentration of compound required to give complete inhibition of bacterial growth. All values were determined in triplicates.

ICL enzyme assay

Isocitrate lyase activity was determined at 37 °C by measuring the formation of glyoxylate-phenylhydrazone at 324 nm. The reaction mixture contains 100 μ L of 0.5 mM potassium phosphate buffer, 1.2 μ L of 1 mM magnesium chloride, 24 μ L of 100 mM 2-mercaptoethanol, 8 μ L of 100 mM phenylhydrazine hydrochloride, 6 μ L of 50 mM trisodiumisocitric acid, and ICL enzyme (usually 3 to 6 μ L). This mixture is made up to 200 μ L with MilliQ water. At the end of the 10th minute, this reaction mixture is made up to 1 mL and UV absorbance is measured at 324 nm, which serves as a control. For the test compounds, 3 μ L of 100 mM 3-NPA was used; and in case of the candidate molecules, 10 μ L of 10 mM concentration added with the above-mentioned reaction mixture. At the end of the 10th minute, this reaction mixture is made up to 1 mL and UV absorbance is measured at 324 nm, which serves as a test. The % inhibition is calculated by the formulae control absorbance minus test absorbance divided by control absorbance multiplied by 100.

Docking methods

The crystal structure of MTB ICL with bound inhibitor, bromopyruvate taken from the Protein Data Bank (PDB entry 1F8M) was used for docking. Before running the docking simulation, the bound inhibitor

was removed from the active site of the enzyme. Using the 'protein preparation wizard' in Schrödinger MAESTRO software, the bond order was assigned for all atoms of the receptor, hydrogen atoms were added, and all the water molecules were removed. The protein was minimized using the optimized potentials for liquid simulations (OPLS) force field to 0.3 Å root-mean-square deviation (rmsd) by keeping the protein backbone constrained. Docking was carried out using MolDock (41). The bond order was assigned for all atoms of the ligand, hydrogen atoms were added, and flexible torsional bonds in the ligands were assigned. Similarly to assign flexible torsional bonds in protein, protein preparation tool was used. Sidechain flexibility with default tolerance was given during docking run to amino acid residues within the 15 Å radius from the center of the bound ligand. Grid was generated with a resolution of 0.30 Å, considering the default bound ligand as the center point with 15 Å radius. Hundred runs, with 5000 iteration for population size of 100 were run with all other default settings using MolDock SE algorithm. The cavity prediction during the search process, allowed for a fast and accurate identification of potential binding modes. The ligand structure was built in Schrödinger Maestro and geometry minimized by applying the OPLS force field.

Cytotoxicity

All the compounds were further examined for toxicity (IC₅₀) in a mammalian Vero cell line till concentrations of 62.5 μ g/mL by serial dilution method. After 72 h of exposure, viability was assessed on the basis of cellular conversion of (3-(4,5-Dimethylthiazol-2-yl)-2,5-diphenyltetrazolium bromide (MTT) into a formazan product using the Promega Cell Titer 96 non-radioactive cell proliferation assay.

In vivo studies

One compound was tested for efficacy against MTB at a dose of 25 mg/kg in 6-week-old female CD-1 mice six per group. In this model, the mice were infected intravenously through caudal vein approximately 10^7 viable *M. tuberculosis* ATCC 35801. Drug treatment by intra peritoneal route began after 10 days of inoculation of the animal with microorganism and continued for 10 days. After 35 days post infection, the spleens and right lungs were aseptically removed and ground in a tissue homogenizer, the number of viable organisms was determined by serial 10-fold dilutions and subsequent inoculation onto 7H10 agar plates. Cultures were incubated at 37 °C in ambient air for 4 weeks prior to counting. Bacterial counts were measured and compared with the counts from negative controls (vehicle treated) in lung and in spleen.

Acknowledgments

The authors are thankful to University Grant Commission [F. No. 36-61/2008 (SR)], Government of India for their financial assistances.

References

1. World Health Organization. (2008) Global TB Control Report. World Health Organization, Geneva, Switzerland.

2. Zhang Y. (2005) The magic bullets and tuberculosis drug targets. *Annu Rev Pharmacol Toxicol*;45:529–564.
3. Zhang Y., Mitchison D. (2003) The curious characteristics of pyrazinamide: a review. *Int J Tuberc Lung Dis*;7:6–21.
4. Kumar R.R., Perumal S., Senthilkumar P., Yogeeswari P., Sriram D. (2008) Discovery of antimycobacterial spiro-piperidin-4-ones: an atom economic, stereoselective synthesis, and biological intervention. *J Med Chem*;51:5731–5735.
5. Dinakaran M., Senthilkumar P., Yogeeswari P., China A., Nagaraja V., Sriram D. (2008) Synthesis, antimycobacterial activities and phototoxic evaluation of 5H-thiazolo[3,2-a]quinoline-4-carboxylic acid derivatives. *Med Chem*;4:482–491.
6. Dinakaran M., Senthilkumar P., Yogeeswari P., China A., Nagaraja V., Sriram D. (2008) Novel ofloxacin derivatives: synthesis, antimycobacterial and toxicological evaluation. *Bioorg Med Chem Lett*;18:1229–1236.
7. Senthilkumar P., Dinakaran M., Banerjee D., Devakaram R.V., Yogeeswari P., China A., Nagaraja V. (2008) Synthesis and antimycobacterial evaluation of newer 1-cyclopropyl-1,4-dihydro-6-fluoro-7-(substituted secondary amino)-8-methoxy-5-(sub)-4-oxoquinoline-3-carboxylic acids. *Bioorg Med Chem*;16:2558–2569.
8. Dinakaran M., Senthilkumar P., Yogeeswari P., China A., Nagaraja V., Sriram D. (2008) Antimycobacterial activities of novel 2-(sub)-3-fluoro/nitro-5,12-dihydro-5-oxobenzothiazolo[3,2-a]quinoline-6-carboxylic acid. *Bioorg Med Chem*;16:3408–3418.
9. Dinakaran M., Senthilkumar P., Yogeeswari P., China A., Nagaraja V., Sriram D. (2008) Antimycobacterial and phototoxic evaluation of novel 6-fluoro/nitro-4-oxo-7-(sub)-4H-[1,3]thiazeto[3,2-a]quinoline-3-carboxylic acid. *Int J Antimicrob Agents*;31:337–344.
10. Sriram D., Senthilkumar P., Dinakaran M., Yogeeswari P., China A., Nagaraja V. (2007) Antimycobacterial activities of novel 1-(cyclopropyl/tert-butyl/4-fluorophenyl)-1,4-dihydro-6-nitro-4-oxo-7-(substituted secondary amino)-1,8-naphthyridine-3-carboxylic acid. *J Med Chem*;50:6232–6239.
11. Sriram D., Yogeeswari P., Dinakaran M., Thirumurugan R. (2007) Antimycobacterial activity of novel 1-(5-cyclobutyl-1,3-oxazol-2-yl)-3-(sub)phenyl/pyridylthiourea endowed with high activity toward multi-drug resistant tuberculosis. *J Antimicrob Chemother*;59:1194–1196.
12. Kumar R.R., Perumal S., Senthilkumar P., Yogeeswari P., Sriram D. (2007) An atom efficient, solvent-free, green synthesis and antimycobacterial evaluation of 2-amino-6-methyl-4-aryl-8-[(E)-arylmethylidene]-5,6,7,8-tetrahydro-4H-pyrano[3,2-c]pyridine-3-carbonitriles. *Bioorg Med Chem Lett*;17:6459–6462.
13. Sriram D., Yogeeswari P., Thirumurugan R., Pavana R.K. (2006) Discovery of newer antitubercular oxazolyl thiosemicarbazones. *J Med Chem*;49:3448–3450.
14. Vedejs E., Marth C.F. (1988) Mechanism of the Wittig reaction: the role of substituents at phosphorus. *J Am Chem Soc*;110:3948–3958.
15. Kangani C.O., Master H.E. (1998) Preparation of 1-aminoanthraquinone-2-carbohydrazide, 1,3,4-oxadiazoles, pyrazoles, pyrimidines and phthalazines. *Ind J Chem*;37:778–783.
16. National Committee for Clinical Laboratory Standards. (1995) Antimycobacterial Susceptibility Testing for *Mycobacterium tuberculosis*. Proposed standard M24-T. Villanova, PA:National Committee for Clinical Laboratory Standards.
17. Katoch V.M. (2004) Infections due to non-tuberculous mycobacteria (NTM). *Ind J Med Res*;120:290–304.
18. Schreiber J., Burkhardt U., Rusch-Gerdes S., Amthor M., Richter E., Zugehor M., Rosahl W., Ernst M. (2001) Non-tubercular mycobacterial infection of the lungs due to *Mycobacterium smegmatis*. *Pneumologie*;55:238–243.
19. Geiss H.K., Feldhues R., Niemann S., Nolte O., Rieker R. (2005) Landouzy septicemia (sepsis tuberculosa acutissima) due to *Mycobacterium microti* in an immunocompetent man. *Infection*;33:393–396.
20. Hachem R., Raad I., Rolston K.V., Whimbey E., Katz R., Tarrand J., Libshitz H. (1996) Cutaneous and pulmonary infections caused by *Mycobacterium vaccae*. *Clin Infect Dis*;23:173–175.
21. Spiegl P.V., Feiner C.M. (1994) Cutaneous and pulmonary infections caused by *Mycobacterium vaccae*. *Foot Ankle Int*;15:680–683.
22. O' Brien R.J., Geiter L.J., Snider D.E. (1987) The epidemiology of nontuberculous mycobacteria disease in the United States; results from a national survey. *Am Rev Respir Dis*;135:1007–1014.
23. Tabatabaei N., Stout J., Goldschmidt-Clermont P., Murdoch D. (2007) Central nervous system infection and cutaneous lymphadenitis due to *Mycobacterium kansasii* in an immunocompetent patient. *Infection*;35:291–294.
24. Xie Z., Siddiqi N., Rubin E.J. (2005) Differential antibiotic susceptibilities of starved *Mycobacterium tuberculosis* isolates. *Antimicrob Agents Chemother*;49:4778–4780.
25. Wayne L.G., Sohaskey C.D. (2001) Non-replicating persistence of *Mycobacterium tuberculosis*. *Ann Rev Microbiol*;55:139–163.
26. Betts J.C., Lukey P.T., Robb L.C., Mc Adam R.A., Duncan K. (2002) Evaluation of a nutrient starvation model of *Mycobacterium tuberculosis* persistence by gene and protein expression profiling. *Mol Microbiol*;43:717–731.
27. Hu Y., Coates A.R.M., Mitchison D.A. (2003) Sterilizing activities of fluoroquinolones against rifampin-tolerant populations of *Mycobacterium tuberculosis*. *Antimicrob Agents Chemother*;47:652–657.
28. Mc Dermott W. (1958) Microbial persistence. *Yale J Biol Med*;30:257–291.
29. Zhang Y. (2004) Persistent and dormant tubercle bacilli and latent tuberculosis. *Front Biosci*;9:1136–1156.
30. O' Brien R.J., Nunn P.P. (2001) The need for new drugs against tuberculosis. Obstacles, opportunities, and next steps. *Am J Respir Crit Care Med*;163:1055–1058.
31. Murphy D.J., Brown J.R. (2008) Novel drug target strategies against *Mycobacterium tuberculosis*. *Curr Opin Microbiol*;11:422–427.
32. Mc Kinney J.D. (2000) Persistence of *Mycobacterium tuberculosis* in macrophages and mice requires the glyoxylate shunt enzyme isocitrate lyase. *Nature*;406:735–738.
33. Glickman M.S. (2000) A novel mycolic acid cyclopropane synthetase is required for cording, persistence, and virulence of *Mycobacterium tuberculosis*. *Mol Cell*;5:717–727.
34. Dahl J.L. (2003) The role of RelMtb-mediated adaptation to stationary phase in long-term persistence of *Mycobacterium tuberculosis* in mice. *Proc Natl Acad Sci USA*;100:10026–10031.
35. Park H.D. (2003) Rv3133c/dosR is a transcription factor that mediates the hypoxic response of *Mycobacterium tuberculosis*. *Mol Microbiol*;48:833–843.

36. Bentrup K.H.Z., Miczak A., Swenson D.L., Russell D.G. (1999) Characterization of activity and expression of isocitrate lyase in *Mycobacterium avium* and *Mycobacterium tuberculosis*. *J Bacteriol*;181:7161–7167.
37. Bai B., Xie J.P., Yan J.F., Wang H., Hu C. (2006) A high throughput screening approach to identify isocitrate lyase inhibitors from traditional chinese medicine sources. *Drug Dev Res*;67:818–823.
38. Sharma V., Sharma S., Kerstin H.B., McKinney J.D., Russell D.G., Jacobs W.R., Sacchettini J.C. (2000) Structure of isocitrate lyase, a persistence factor of *Mycobacterium tuberculosis*. *Nat Struct Biol*;8:633–668.
39. Gundersen L.L., Nissen-Meyer J., Spilsberg B. (2002) Synthesis and antimycobacterial activity of 6-arylpurines: the requirements for the N-9 substituent in active antimycobacterial purines. *J Med Chem*;45:1383–1386.
40. Sriram D., Yogeeswari P., Basha S.J., Radha D.R., Nagaraja V. (2005) Synthesis and antimycobacterial evaluation of various 7-substituted ciprofloxacin derivatives. *Bioorg Med Chem*;13: 5774–5778.
41. Thomsen R., Christensen M.H. (2006) MolDock: a new technique for high-accuracy molecular docking. *J Med Chem*;49:3315–3321.